

Relations between Potential Energy, Electronic Chemical Potential, and Hardness Profiles

Gloria I. Cárdenas-Jirón, Soledad Gutiérrez-Oliva, Junia Melin, and Alejandro Toro-Labbé*

Centro de Mecánica Cuántica Aplicada, Departamento de Química, Facultad de Ciencias, Universidad de Chile, Casilla 653, Santiago, Chile

Received: November 20, 1996; In Final Form: February 20, 1997[⊗]

In recent papers we defined a theoretical frame aimed at characterizing the hardness and potential energy profiles along a reduced reaction coordinate (ω) varying from 0 to 1. In this paper we generalize that model to propose a global procedure that allows one to consider simultaneously the evolution of the potential energy (V) in connection with that of the electronic chemical potential (μ) and the molecular hardness (η). Important results have been obtained: (a) the potential energy profile can be expressed in terms of the μ and η profiles through an equation which is analogous to that used by Parr and Pearson to demonstrate the HSAB principle; (b) the chemical potential along ω is in turn written in terms of the hardness profile, an equation which is analogous to that proposed by the same authors to quantify the electron transfer induced by a chemical potential gradient; and (c) useful expressions for the activation properties have been derived. As an illustration we study the *trans* \rightleftharpoons *cis* isomerization of diimide, a reaction that may occur through either an internal rotation or an inversion mechanism. The most relevant result concerning the chemical system is that for both mechanisms the principle of maximum hardness holds even though the electronic chemical potential strongly varies along the reaction coordinates. Our analysis suggests that if a system is constrained to choose among different reaction paths connecting two stable states, it will prefer the one presenting a minimum chemical potential.

1. Introduction

Density functional theory (DFT), a theory based upon the ground state electronic density distribution of atoms and molecules, has provided the theoretical basis for concepts like electronic chemical potential (μ) and molecular hardness (η).^{1–6} The electronic chemical potential characterizes the escaping tendency of electrons from the equilibrium system, whereas molecular hardness can be seen as a resistance to charge transfer. Both μ and η are global properties of the system.

It has been recently shown that the hardness profile along a reaction coordinate is quite useful to study the progress of chemical reactions.⁷ In this context, the relation between hardness and energy profiles appears to be especially important for characterizing transition states.^{8,9} The hardness profile passes through a minimum near or at the transition state for different types of reactions, although some symmetric stretching modes of deformation do not always correspond to extremum values of hardness at the equilibrium conformation.^{7–10} In connection with this, the principle of maximum hardness (PMH) asserts that molecular systems at equilibrium tend to states of high hardness;⁴ transition states should therefore present a minimum value of hardness. It follows that the combination of the PMH with the Hammond postulate¹¹ constitutes a quite powerful tool for a qualitative characterization of transition states.⁹ Parr and Chattaraj¹² showed that the PMH holds under the constraints that the external potential and the electronic chemical potential must remain constant upon distortion of the molecular structure. However, the PMH seems to be valid even under less restrictive conditions than the ones stated above. Relaxation of the constraints seems to be permissible, and in particular, it has been found that the electronic chemical potential is not always constant along a reaction coordinate.^{9,13–15}

As far as the electronic chemical potential is concerned, most studies have been performed within the frame of the constraints of the PMH; they have been confined to evaluate μ under small distortions of the molecular structure with the result that it remains reasonably constant.^{13–15} However, few molecules presenting torsional isomerization reactions show a non-negligible variation of μ along a reaction coordinate.^{7,9} It is thus of interest to study the variation of this property in connection with the potential energy and hardness profiles. To do so we propose in this paper a theoretical framework that provides analytic expressions for the evolution of these global properties along a reaction coordinate and allows direct connections among them.

Due to the above commented fact that most studies on the variation of the electronic chemical potential concluded that it remains constant upon distortions of the molecule, validating in this way the PMH, we choose to illustrate our model relating energetic and electronic properties with the study of two different isomerization mechanisms in a system where the energy barriers separating two stable states are sufficiently high to expect strong variations of the chemical potential and hardness. A challenging process for our purposes is the *trans* \rightleftharpoons *cis* isomerization reaction of diimide (HN=NH) which can occur through internal rotation about the double bond or through inversion at one nitrogen atom. Diimide (or diazene) is a short lived species that has been identified as one of the decomposition products of the hydrazoic acid and hydrazine reaction.¹⁶ It is usually employed in the selective reduction of nonpolar bonds and as ligands in transition metal complexes. Although N₂H₂ cannot be isolated under ordinary conditions, its infrared spectrum has been studied by many authors.^{17–20} From a theoretical viewpoint, diimide has also been studied by many authors, and the most relevant conclusion that concerns this paper is that the barriers associated with the different isomerization mechanisms have been found to be about 46–60 kcal/

[⊗] Abstract published in *Advance ACS Abstracts*, May 15, 1997.

mol,^{21–26} high enough to expect a strong variation of the electronic properties along the different reaction pathways.

2. Theory

Energy, Chemical Potential, and Hardness Profiles. We start by defining a reduced reaction coordinate ω , which can be related to the actual reaction coordinate through a scaling procedure under the condition that it varies from 0 (initial state) to 1 (final state) with $\omega = 0.50$ at midway between the reference states. These are characterized by the extremum values of ω , in the present case the *trans* and *cis* conformations that correspond to $\omega = 0$ and $\omega = 1$, respectively. The reduced coordinate can therefore be viewed as a measure of the reaction progress going from reactants ($\omega = 0$) to products ($\omega = 1$), passing through a transition state.

The potential energy representing a *trans* \rightleftharpoons *cis* isomerization process, following the rotation or inversion pathways, is given by^{8,9}

$$V(\omega) = K_V f(\omega) + \omega \Delta V^0 \quad (1)$$

where $K_V = (k_t + k_c)$ with k_t and k_c the torsional force constants associated with the reference conformations (for the inversion mechanism they will correspond to bending force constants) and $\Delta V^0 = (V(1) - V(0))$ is the energy difference between those conformations. In eq 1, $f(\omega)$ is a function which must be symmetric about $\omega = 1/2$ where it is maximal. Many conveniently normalized functions qualify with this requirement; they all must have the same behavior about $\omega = 1/2$, and therefore they only may differ in their wings. Due to its thermodynamic implications, an appealing function that satisfies the above requirement is $f(\omega) = -[\omega \ln \omega + (1 - \omega) \ln(1 - \omega)]$; however, the function $f(\omega) = \omega(1 - \omega)$, that came out from a Fourier expansion of the torsional potential, has been used in our previous papers^{8,9} and will be used here to rationalize the *ab initio* results of the internal rotation and inversion of diimide.

Since the electronic chemical potential and molecular hardness are global properties of the system, they can be written in terms of the same analytic form used for the potential energy in eq 1. Therefore we have

$$\mu(\omega) = K_\mu f(\omega) + \omega \Delta \mu^0 \quad (2)$$

and

$$\eta(\omega) = K_\eta f(\omega) + \omega \Delta \eta^0 \quad (3)$$

In eqs 2 and 3 the parameters $\Delta \mu^0$, $K_\mu = (\mu_t + \mu_c)$ and $\Delta \eta^0$, $K_\eta = (\eta_t + \eta_c)$, respectively, have the same meaning that ΔV^0 , K_V , has for $V(\omega)$. The parameters of eqs 1–3 will be determined following a prescription given in our previous works^{8,9} and briefly reviewed in section 3.

The $\{\mu, V\}$ Representation. The above equations show that $V(\omega)$, $\mu(\omega)$, and $\eta(\omega)$ are connected through the function $f(\omega)$. Using eq 2 to express $f(\omega)$ in terms of the electronic chemical potential allows one to define with eq 1 a potential energy $V_\eta(\omega)$, where the index is indicating that it formally considers the hardness as being constant

$$V_\eta(\omega) = \omega \Delta V^0 + Q_\eta (\mu(\omega) - \omega \Delta \mu^0) \quad (4)$$

where $Q_\eta = K_V/K_\mu$. In Figure 1a we show a schematic view of the progress of a chemical reaction in the $\{\mu, V\}$ space; the arrows are indicating the sense of the reaction (from *trans* to *cis* passing through the transition state). The parameter Q_η appearing in eq 4 can be independently determined by drawing

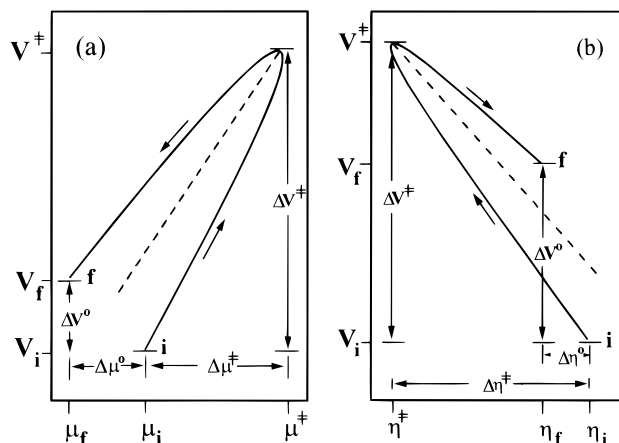


Figure 1. Schematic view of the 2D representations of the evolution of a chemical reaction in the $\{\mu, V\}$ and $\{\eta, V\}$ spaces. The arrows indicate the sense of the reaction going from the initial state (i) to the final state (f) and passing through the transition state.

a straight line intersecting the parabolic function, a straight line that is rigorously obtained through the rectilinear diameters law (RDL) usually invoked to determine critical constants in thermodynamics.⁸ It can be noticed that for reactions presenting small values of ΔV^0 and $\Delta \mu^0$ the parabolic form of Figure 1a reduces to a straight line with slope Q_η .

The $\{\eta, V\}$ Representation. When the electronic chemical potential remains constant along ω , it is interesting to express $V(\omega)$ in terms of $\eta(\omega)$. This allows to connect concepts like the PMH and the Hammond postulate.⁹ Following the same procedure we used to obtain $V_\eta(\omega)$, the combination of eqs 1 and 3 leads to definition of $V_\mu(\omega)$

$$V_\mu(\omega) = \omega \Delta V^0 + Q_\mu (\eta(\omega) - \omega \Delta \eta^0) \quad (5)$$

with $Q_\mu = K_V/K_\eta$. Equation 5 was discussed in our previous papers with the result that Q_μ should be negative in attention to the PMH.^{8,9} In Figure 1b is displayed the progress of the chemical reaction in the $\{\eta, V\}$ space. Isomerization processes going from one stable conformation to another stable conformation lead to a clockwise *trans* \rightarrow transition state \rightarrow *cis* path in the $\{\eta, V\}$ diagram, as indicated by the arrows in Figure 1b. As in the precedent case, the straight line with slope Q_μ that bisects the parabola is obtained using the RDL.

It should be noted that the $\{\mu, V\}$ and $\{\eta, V\}$ diagrams show that a necessary condition for consistency between $V(\omega)$, as defined in eq 1, $V_\eta(\omega)$, and $V_\mu(\omega)$ is that $V_\eta(\omega) = V_\mu(\omega) = V(\omega)$ for all ω . In particular, the energy barrier separating two stable conformations can be derived from any of the equations defining the potential energy function.

The $\{\eta, \mu\}$ Representation. From the fundamental DFT it has been shown that at equilibrium systems attain a given chemical potential, which can be written in terms of the properties of isolated reactants.^{4,5,27} For a $A + B \rightarrow AB$ type of reaction, Parr and Pearson showed that the number of electrons (ΔN) transferred between A and B is given by:²

$$\Delta N = \frac{(\mu_B - \mu_A)}{(\eta_B + \eta_A)} \quad (6)$$

This equation states that the difference in chemical potential drives the electron transfer, whereas the sum of the individual hardnesses inhibits it.^{4,5,27} Our model that considers reactants and products as different chemical species trapped on local potential wells leads to the following expression for the

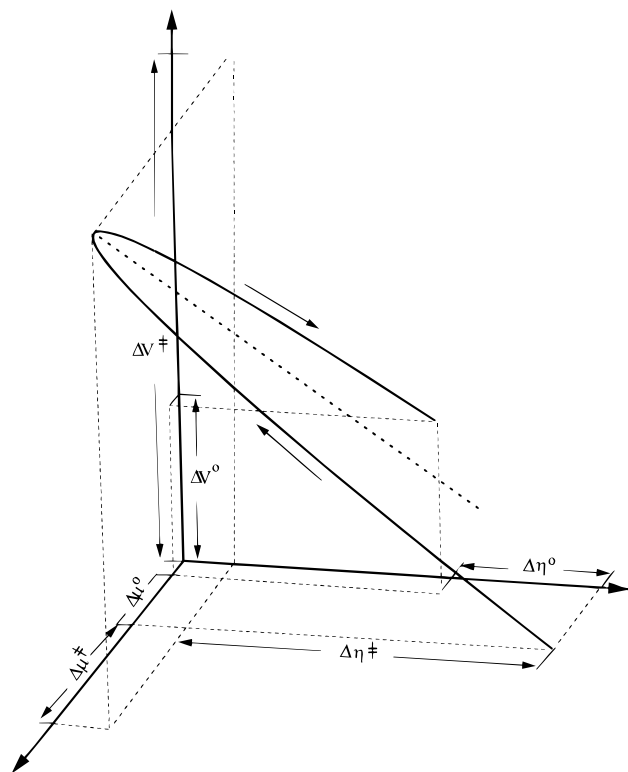


Figure 2. Schematic view of the 3D representation of the evolution of the potential energy in the $\{\mu, \eta, V\}$ space.

electronic chemical potential in terms of the molecular hardness

$$\mu(\omega) = \omega\Delta\mu^0 + Q(\eta(\omega) - \omega\Delta\eta^0) \quad (7)$$

with $Q = Q_\mu/Q_\eta$, given by

$$Q = \frac{\mu(\omega) - \omega\Delta\mu^0}{\eta(\omega) - \omega\Delta\eta^0} \quad (8)$$

The minus signs appearing in eq 8 are due to the fact that we are dealing with relative values of μ and η . Since all values are relative to those of the *trans* conformations, negative values of $\eta(\omega)$ are allowed, and so eq 8 is well-defined in the range $0 < \omega < 1$. On the other hand, we have checked the behavior of Q along ω and found that it is constant with singularities at $\omega = 0$ and $\omega = 1$ because μ and η are defined with respect to their values at $\omega = 0$. It is interesting to compare, at least qualitatively, eqs 6 and 8. It follows that Q might be related to some charge redistributed among the atoms in the molecule during the chemical reaction, and the hardness appears to be acting as a resistance to that redistribution.

The $\{\mu, \eta, V\}$ Representation. When both μ and η vary with ω it is then possible to obtain an alternative and more general expression for the potential energy. We take the arithmetic average of eqs 4 and 5 to obtain

$$\begin{aligned} V(\omega) &\equiv \frac{1}{2}(V_\eta(\omega) + V_\mu(\omega)) \\ &= \omega\Delta V^0 + \frac{1}{2}Q_\eta(\mu(\omega) - \omega\Delta\mu^0) + \\ &\quad \frac{1}{2}Q_\mu(\eta(\omega) - \omega\Delta\eta^0) \quad (9) \end{aligned}$$

Figure 2 shows how the reaction progress looks like in the $\{\mu, \eta, V\}$ space. As in the previous diagrams, the parabolic form can be rationalized with the help of the 3D RDL, and it reduces to a 3D straight line in the case of symmetric reactions.

It is interesting to note that eq 9 is analogous to

$$E = E^0 + \Delta N\mu + \frac{1}{2}(\Delta N)^2\eta + \dots \quad (10)$$

which, according to Parr and Pearson,² is the energy of an atom in a molecule with electrons flowing from or to that atom and keeping the external potential (v) constant. Changes in N and v lead to a more general expression for the energy that includes the Fukui function and allows discussion of energy in terms of frontier orbital theories of chemical reactivity.^{5,27} Again, the term to term comparison of eqs 9 and 10 suggests that Q_η and Q_μ are related in some way to the change of the electronic charge (ΔN) when going from reactants to products.

Another evidence pointing at the sense that eq 9 correctly contains the μ and η dependence of the energy is that it is very similar to

$$\Delta E = \Delta E^0 + \frac{1}{2}a\Delta\mu^0 + \frac{1}{2}b\Delta\eta^0 \quad (11)$$

which we have derived in the context of the thermochemistry of formation of hydrogen thioperoxide (HSOH) from its radical and ionic fragments.²⁸

The above characterization of a chemical reaction presents the advantage of giving simultaneous information about the change of energy and electronic properties along the reaction coordinate. In fact, since the change in electronic properties is related to the reaction mechanism, eq 9 is connecting the energetic and mechanistic aspects of a chemical reaction. Our approach appears to be complementary to other approaches aimed at following the course of chemical reactions. For example, in the frame of the time-dependent DFT, Chattaraj and Nath have studied the electronegativity (the negative of the chemical potential) and hardness dynamics in chemical reactions,^{29,30} obtaining important insights that help characterize the temporal evolution of electronic properties. An interesting extension of this work would be to study the behavior of eq 9 under the temporal evolution of V , μ , and η .

A Thermodynamic-like Approach. Equation 9 suggests that it should be possible to build up a thermodynamic-like approach connecting the three properties we are studying here. Let us write the potential energy in the $\{\mu, \eta, V\}$ space considering the electronic chemical potential and the molecular hardness as independent variables. The differential expression of $V(\mu, \eta)$ is

$$dV = \left(\frac{\partial V}{\partial \mu}\right)_\eta d\mu + \left(\frac{\partial V}{\partial \eta}\right)_\mu d\eta \quad (12)$$

where we took $dV = (V(\omega) - \omega\Delta V^0)$. The slopes appearing in the above equation are obtained from eqs 4 and 5

$$\left(\frac{\partial V}{\partial \mu}\right)_\eta \equiv \frac{1}{2} \left(\frac{dV_\eta}{d\mu}\right) = \frac{1}{2} \frac{(V_\eta(\omega) - \omega\Delta V^0)}{(\mu(\omega) - \omega\Delta\mu^0)} = \frac{1}{2} Q_\eta \quad (13)$$

and

$$\left(\frac{\partial V}{\partial \eta}\right)_\mu \equiv \frac{1}{2} \left(\frac{dV_\mu}{d\eta}\right) = \frac{1}{2} \frac{(V_\mu(\omega) - \omega\Delta V^0)}{(\eta(\omega) - \omega\Delta\eta^0)} = \frac{1}{2} Q_\mu \quad (14)$$

Equation 12 can now be rewritten as

$$dV = \frac{1}{2}Q_\eta d\mu + \frac{1}{2}Q_\mu d\eta \quad (15)$$

Assuming now that Q_η and Q_μ are variables and the pairs $\{Q_\eta, \mu\}$ and $\{Q_\mu, \eta\}$ are conjugated to one another, appropriate Legendre

transformations lead to

$$U(\omega) = \omega\Delta U^0 - \frac{1}{2}(\mu(\omega) - \omega\Delta\mu^0) dQ_\eta - \frac{1}{2}(\eta(\omega) - \omega\Delta\eta^0) dQ_\mu \quad (16)$$

where after the transformation the energy U is defined as $U=V - (Q_\eta\mu + Q_\mu\eta)/2$. Therefore, if the parameters Q_η and Q_μ are allowed to vary, then we obtain an equation that is homogeneous to eq 10, the Parr and Pearson expression used to explain a formation process of a molecule from the isolated atoms.²

Activation Properties. To determine the position of the transition state associated with the potential $V(\omega)$ we make use of the function $f(\omega) = (1 - \omega)\omega$ in eq 1 such that $(dV/d\omega)_{\omega=\beta} = 0$, thus obtaining the position β in terms of the potential energy parameters:

$$\beta = \frac{1}{2} + \frac{\Delta V^0}{2K_V} \quad (17)$$

This equation is in fact a quantitative formulation of the Hammond postulate: if $\Delta V^0 > 0$ then $\beta > 1/2$ and the transition state is closer to products, whereas if $\Delta V^0 < 0$ then $\beta < 1/2$ and the transition state is closer to reactants.¹¹ Putting β in eq 1 yields to the following expression for the activation energy:

$$\Delta V^\ddagger \equiv V(\beta) = \frac{1}{4}K_V + \frac{1}{2}\Delta V^0 + \frac{(\Delta V^0)^2}{4K_V} \quad (18)$$

Note that this equation is similar to the one derived by Marcus in his theory of electron transfer in solution.³¹ The parameter β is known as the Brønsted coefficient, and physically it represents a measure of the degree of resemblance of the transition state with respect to the product. The Brønsted coefficient is often used to quantify the empirical concepts of *reactant-like* ($0 \leq \beta \leq 1/2$) and *product-like* ($1/2 \leq \beta \leq 1$) transition state.^{8,9,32-34} By evaluating eq 9 in $\omega = \beta$ we obtain an alternative expression for the activation energy, now in terms of the activation chemical potential ($\Delta\mu^\ddagger \equiv \mu(\beta)$) and the activation hardness ($\Delta\eta^\ddagger \equiv \eta(\beta)$):

$$\Delta V^\ddagger = \beta\Delta V^0 + \frac{1}{2}Q_\eta(\Delta\mu^\ddagger - \beta\Delta\mu^0) + \frac{1}{2}Q_\mu(\Delta\eta^\ddagger - \beta\Delta\eta^0) \quad (19)$$

This equation connecting the three activation properties might provide new interpretations of the nature of activation energies, and certainly it may help to give new insights about reaction mechanisms. It has been found in different types of reactions that μ and η pass through an extrema at β or very near to it;⁸⁻¹⁰ this ensures that eq 19 produces reliable values of potential barriers from the knowledge of activation electronic properties.

The activation chemical potential is obtained by evaluating eq 4 at $\omega = \beta$, thus obtaining:

$$\Delta\mu^\ddagger = \beta\Delta\mu^0 + \frac{1}{Q_\eta}(\Delta V^\ddagger - \beta\Delta V^0) \quad (20)$$

The electronic chemical potential is expected to be smaller than the total energy; it then follows that $|Q_\eta| \geq 1$ to have $\Delta\mu^\ddagger \leq \Delta V^\ddagger$.

On the other hand, the activation hardness is obtained from eq 5:

$$\Delta\eta^\ddagger = \beta\Delta\eta^0 + \frac{1}{Q_\mu}(\Delta V^\ddagger - \beta\Delta V^0) \quad (21)$$

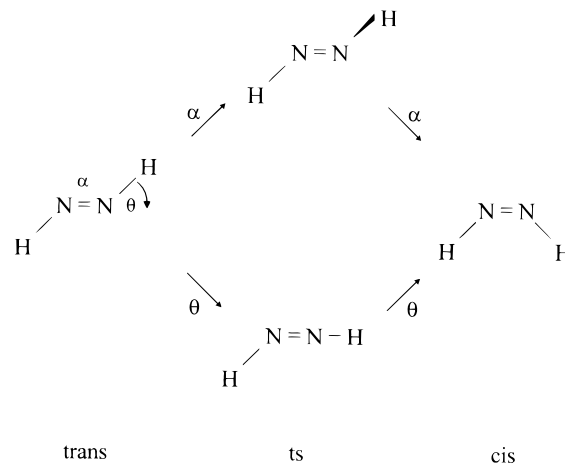


Figure 3. Rotation and inversion mechanisms for the isomerization of diimide.

It is proportional and opposite (Q_μ is negative) to the activation energy. The above equation was derived in slightly different terms in our previous papers and was used with success in the determination of activation hardnesses for rotational isomerization processes.^{8,9} It is important to mention that Zhou and Parr also found proportionality between $\Delta\eta^\ddagger$ and ΔV^\ddagger in electrophilic aromatic substitution processes.³⁵ Finally, we note that alternative expressions for the electronic activation properties in terms of the potential parameters K_V and ΔV^0 can be obtained by using in the above equations the definition of β and ΔV^\ddagger (eqs 17 and 18, respectively).

3. Calculations

The above described model relating the profiles of the potential energy, electronic chemical potential, and molecular hardness is now used to rationalize *ab initio* calculations of the *trans* \rightleftharpoons *cis* isomerization of the HN=NH molecule, isomerization that can occur through a rotation or an inversion mechanism, as shown in Figure 3. Both are important mechanisms in chemistry, and their study constitutes a challenge to test our model in different reaction pathways where the electronic chemical potential is expected to change strongly along the reaction coordinates. The isomerization of diimide has been widely studied, and high-level calculations estimating barrier heights and structural properties are currently available.^{25,26} It has been established that since the inversion mechanism leads to a closed shell transition state whereas the internal rotation yields to a biradical transition state, sophisticated calculations going beyond the self-consistent field (SCF) energy are necessary to have a common theoretical method allowing proper comparisons among these structures.^{25,26} However, since the aim of this paper is mainly methodological, we will concentrate our analysis to $\mu(\omega)$ and $\eta(\omega)$ in terms of their relationships with $V(\omega)$ and all properties will be calculated in the frame of the Hartree-Fock SCF theory, without paying further attention to the accuracy of the numerical values obtained. Therefore, our numerical results should be taken on a qualitative basis, they will be used to illustrate the theoretical procedure depicted in section 2, keeping in mind that for quantitative purposes they may need further improvements.

The Reaction Coordinates. We start by defining the reduced reaction coordinate for the different reaction mechanisms. The coordinate ω is related to the torsional (dihedral) angle α through^{8,9} $\omega(\alpha) = (1 - \cos \alpha)/2$ with ω varying from 0 ($\alpha = 0$) to 1 ($\alpha = \pi$), extrema that indicate the *trans* and *cis* reference conformations, respectively. On the other hand, the inversion mechanism is represented by moving a hydrogen in the NNH

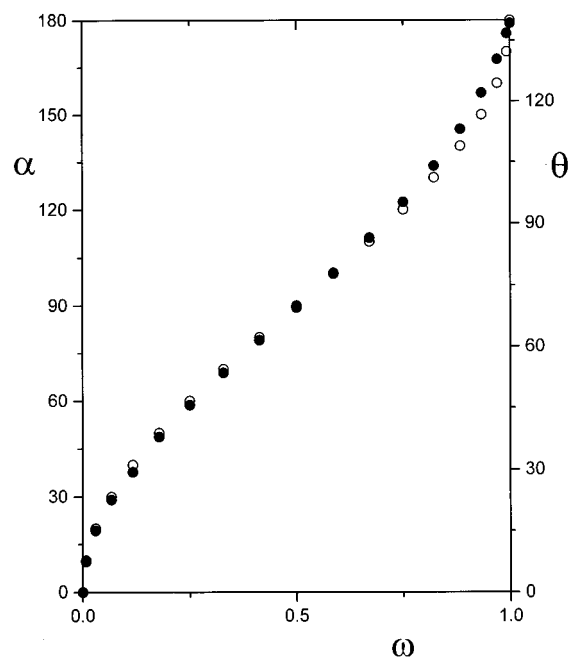


Figure 4. Representation of the rotation (α , open circles) and inversion (θ , filled circles) coordinates (in degrees) in terms of the reduced coordinate ω .

plane; this generates a trajectory defined by the angle θ , as shown in Figure 3. The angle θ goes from 0 (*trans*, $\omega = 0$) to 139.29° (*cis*, $\omega = 1$) and passes through $\theta = 69.65^\circ$ where $\omega = 0.50$. These three values were used to determine $\omega(\theta) = 0.7044 - 0.5255 \cos \theta - 0.1789 \cos^2 \theta$. In Figure 4 we display the evolution of the torsional and inversion coordinates along the reduced variable ω .

Parameters Defining $V(\omega)$, $\mu(\omega)$ and $\eta(\omega)$. The parameters involved in eqs 1–3 were determined following the prescription given in our previous works.^{8,9} It asserts that two energy points at the vicinity of the reference conformations are needed to estimate the curvature of the assumed harmonic potential wells in which the reference conformations are trapped. For the internal rotation we have performed calculations at $\omega = 0$ and $\omega = 0.0076$ ($\alpha = 0^\circ$ and 10° , respectively), leading to determination of k_t , μ_t and η_t . Calculations at $\omega = 0.9924$ and $\omega = 1$ ($\alpha = 170^\circ$ and 180° , respectively) led to k_c , μ_c , and η_c .^{8,9} In the case of the inversion mechanism, calculations at $\omega = 0$ and $\omega = 0.0105$ ($\theta = 0^\circ$ and 10° , respectively) led to k_t , μ_t , and η_t and calculations at $\omega = 0.9715$ and $\omega = 1$ ($\theta = 129.29^\circ$ and 139.29° , respectively) led to k_c , μ_c and η_c . For a more detailed discussion about the procedure we use to numerically obtain the input parameters needed to define $V(\omega)$, $\mu(\omega)$ and $\eta(\omega)$, the reader is referred to our previous papers.^{32–34} In Table 1 are quoted the input parameters necessary to obtain the profiles of these properties along the reaction paths.

Method of Calculation. We have performed calculations at the Hartree–Fock (HF) SCF level with a standard 6-31G** basis set and with full geometry optimization at the points mentioned in the preceding paragraph. The calculations were performed through the Spartan package.³⁶ A recent theoretical study of the diimide isomerization showed that when the isomerization path does not involve breaking and forming bonds, HF and post-HF calculations lead to quite similar results concerning geometric parameters and barrier heights.³⁷ Our results concerning the optimized geometrical parameters of the structures considered in this work are in good agreement with the available experimental data and theoretical results at different levels of calculation.

TABLE 1: Input Data and Activation Properties for the Internal Rotation and Inversion of Diimide^a

input data	rotation	inversion
k_t	78.4445	168.3952
k_c	60.8893	166.8302
$K_V = (k_t + k_c)$	139.3338	335.2254
ΔV^0	6.8166	6.8166
μ_t	20.1673	312.0726
μ_c	51.8500	338.1055
$K_\mu = (\mu_t + \mu_c)$	72.0173	650.1781
$\Delta \mu^0$	-3.6741	-3.6741
η_t	-79.0007	-205.3633
η_c	-107.1526	-259.4150
$K_\eta = (\eta_t + \eta_c)$	-186.1533	-464.7783
$\Delta \eta^0$	0.6137	0.6137
$Q_\eta = K_V/K_\mu$	1.9347	0.5156
$Q_\mu = K_V/K_\eta$	-0.7485	-0.7213
$Q = Q_\mu/Q_\eta$	-0.3869	-1.3990

output data	rotation	inversion
β	0.5245	0.5102
ΔV^\ddagger	38.3251	87.2493
$\Delta \mu^\ddagger$	16.0344	160.6024
$\Delta \eta^\ddagger$	-46.1044	-115.8331

^a The input parameters are given in kcal/mol · rad², and the energies are in kcal/mol.

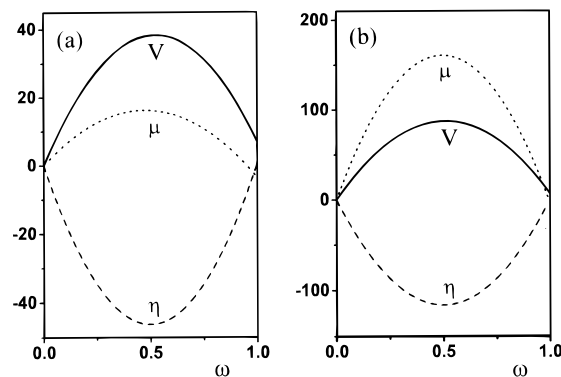


Figure 5. Potential energy, electronic chemical potential, and hardness profiles for the isomerization reaction of diimide following the rotation (a) and inversion (b) mechanisms.

The reference values of electronic chemical potential and molecular hardness were obtained from HF calculations through the operational formulas which come out from the finite-difference approximation.⁵ I and A correspond to the first ionization potential and electron affinity of the molecule and were determined through a Δ SCF procedure. Calculations on ions were performed using the unrestricted Hartree–Fock procedure on the already optimized neutral molecular structure.

4. Results and Discussion

Energy, Chemical Potential, and Hardness Profiles. In Figure 5 we display the curves of potential energy, chemical potential, and hardness along ω for the rotation and inversion mechanisms. We note that for both mechanisms, the potential energy and electronic chemical potential profiles exhibit the same trend with maximum values at the transition state. Opposite to this is the behavior of the hardness, indicating that the PMH is verified for the two isomerization paths. It should be noted that since all values are relative to those of the *trans* conformation, $\eta(\omega)$ may be negative.

The potential barrier associated with the inversion mechanism is higher than the one associated with the internal rotation, indicating that rotation should be the preferred mechanism for isomerization. For the internal rotation, the electronic chemical

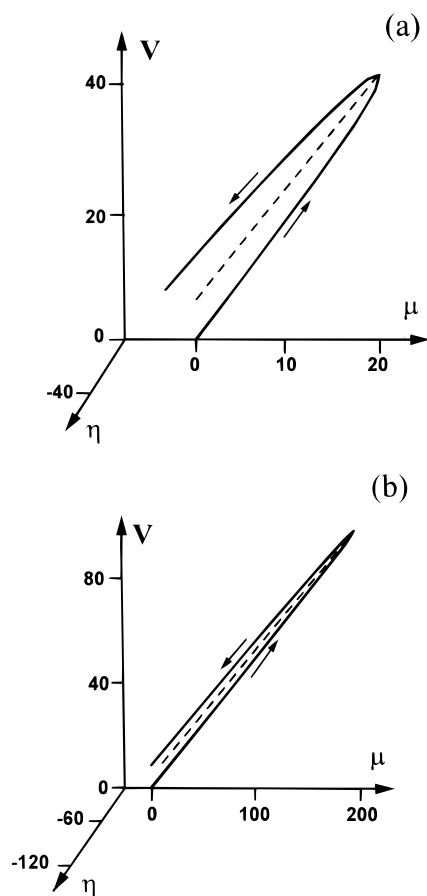


Figure 6. 3D representations of the evolution of the isomerization reaction in the $\{\mu, \eta, V\}$ space following the rotation (a) and inversion (b) mechanisms.

potential along ω is lower than the potential energy, presenting intermediate values between the potential energy and the molecular hardness. This situation is not reproduced for the inversion mechanism, where the μ values are higher than the potential energy values. In both cases the hardness profile behaves similarly although in the inversion mechanism it attains a deeper minimum at the transition state.

A chemical process is driven by μ when this property follows a minimum chemical potential path which, in the present case, corresponds to the rotation mechanism. In this case a delicate balance between potential energy and hardness seems to be present: the chemical potential profile is intermediate between the η and V profiles. In contrast to this, the inversion mechanism presents a chemical potential profile which is even higher than energy profile due to an anomalous value of the parameter Q_η (0.5156) that should be higher than one (see Table 1).

3D Representation of the Isomerization Process. In Figure 6 are displayed the 3D representations of the different isomerization mechanisms studied in this paper. We note that the rotation mechanism is represented by an open parabola, whereas the parabola representing the inversion mechanism is closer to a straight line. It is interesting to mention that projections of the 3D straight lines of Figure 6 onto the $\{\mu, V\}$, $\{\eta, V\}$, and $\{\mu, \eta\}$ planes leads to three 2D straight lines defined through their slopes Q_η , Q_μ , and Q , respectively. These are quasi orthogonal to each other and may be orthogonalized through classical methods. This confirms the assumption we made in performing Legendre transformations on eq 9 that Q_η and Q_μ are conjugated variables of μ and η , respectively. This may be an important result and merits further attention since it suggests

that it should be possible to perform mathematical transformations to express the energy and electronic properties in some $\{Q_\eta, Q_\mu\}$ space. In particular, if orthogonality is verified, then the parabolic forms obtained in the $\{\mu, \eta, V\}$ space suggest that in the $\{Q_\eta, Q_\mu\}$ space we should be able to write $Q_\mu \approx CQ_\eta^2$ and therefore the correspondence between the parameters appearing in eqs 9 and 10, $Q_\eta \leftrightarrow \Delta N$ and $Q_\mu \leftrightarrow \Delta N^2$, seem to be correct, at least qualitatively. Moreover, by defining the origin of the coordinate system at the transition state, it should be possible to determine rules to make the system decide among different reaction paths in terms of the numerical values of Q_η and Q_μ .

On the other hand, in all the representations of the potential energy, electronic chemical potential, and hardness profiles, the inversion mechanism exhibits close linear dependences, which are the characteristic feature of symmetric situations. In this mechanism, the symmetry plane of the molecule is conserved along the reaction coordinate, whereas torsion about the central bond breaks down all symmetry elements of the molecule. This observation may be used to confirm the fact that a reaction path that keeps a symmetry element along it might not necessarily be the preferred direction that follows the system. Such a symmetry element might be considered as unstable, in the sense pointed out by Pearson and Palke.¹³

Activation Properties. In Table 1 are displayed the activation properties we have obtained through eqs 17–21. Note that for the two mechanisms we are studying in this paper the parameter β is showing that transition states are closer to the product than to the reactants, a result that verifies the Hammond postulate ($\Delta V^0 > 0$). On the other hand, relatively good agreement of the value for the rotation barrier, predicted through eq 18, is anticipated on the basis of comparisons with the available literature data at the HF level. For the rotation about the N=N central bond, a value of 38.3 kcal/mol is anticipated which is in good agreement with 37.2 kcal/mol obtained by Cimiriaglia *et al.*²⁵ In contrast to this, for the inversion mechanism, eq 18 predicts a value of 87.2 kcal/mol that is too high when compared to the available literature data.^{25,26,37}

Barrier heights at higher levels of calculation have been recently reported by Cimiriaglia *et al.*²⁶ These authors used different polarized basis sets going beyond Hartree–Fock by means of complete active space–self-consistent field (CAS-SCF) and CIPSI techniques to perform quantitative comparisons of the energy and structures of the different transition states involved in the isomerization mechanisms of diimide. They suggest that both mechanisms are quite competitive. Our estimations for the barrier heights associated with the different reaction mechanisms and the criterium that a reaction must follow a minimum chemical potential path lead us to conclude that rotation would be the preferred mechanism.

Our ΔV^\ddagger values allow one to conclude that while the parameter K_V for the rotational mechanism seems to be quite well-estimated, leading to a reasonably good barrier for internal rotation, the corresponding parameter for the inversion mechanism seems to be overestimated, thus producing a too large barrier to inversion. To quantify the error we have in our calculation of this parameter for inversion, we use the ΔV^\ddagger and ΔV^0 values reported by Cimiriaglia *et al.* (51.7 kcal/mol and 3.15 kcal/mol, respectively) obtained at the CAS-SCF level²⁶ to solve the second-order equation in K_V that can be derived from eq 18. As a result, we obtain $K_V = 243.6$ kcal/mol \cdot rad² that compared with our original estimation of 335.2 kcal/mol \cdot rad² leads to an error of about 27%. Similar effects are expected in our estimation of the remaining parameters associated with the inversion. It is therefore clear that more sophisticated wave

functions will improve quantitatively and qualitatively our results, especially those concerning the inversion mechanism.

5. Summary and Concluding Remarks

In this paper we have proposed a theoretical model aimed at considering simultaneously the evolution of the potential energy, electronic chemical potential, and molecular hardness along a reaction coordinate. The model proposed was used in the study of the *trans* \rightleftharpoons *cis* isomerization reaction of diimide following two different pathways: internal rotation about the double bond or inversion at one nitrogen atom. In both mechanisms the principle of maximum hardness holds even though the electronic chemical potential changes strongly during the chemical reaction.

The analysis presented in this paper suggests that the chemical potential responds to a delicate balance between the potential energy and hardness. In some cases this may lead to a constant chemical potential along the reaction coordinate, although variations are permissible in the range $\eta(\omega) \leq \mu(\omega) \leq V(\omega)$. Our results show that internal rotation is the preferred mechanism for isomerization because it presents the lowest energy barrier and the minimum chemical potential path.

The parameters Q_η , Q_μ , and Q have been qualitatively related to some charge redistributed among the atoms in the molecule during the isomerization process. However, open questions remain. They concern the exact identification of these charges and their eventual use as quantitative indexes to make the system decide among different reactive channels. Since for the isomerization reactions we have studied in this paper only intramolecular charge transfer may occur, it may be redistributed in specific regions of the molecular topology, and therefore the analysis of condensed charges along the reaction coordinate certainly will help identify these parameters. Concerning their use as reactivity indexes, we believe that convenient transformations putting the transition state at the origin of a new coordinate system, the $\{Q_\eta, Q_\mu\}$ space, will allow determination of empirical relations between these parameters, giving insights about this point.

Acknowledgment. The authors are thankful for the financial support from FONDECYT through projects numbered 2950029/95 and 1961021.

References and Notes

- (1) Parr, R. G.; Yang, W. *Annu. Rev. Phys. Chem.* **1995**, *46*, 701.
- (2) Parr, R. G.; Pearson, R. G. *J. Am. Chem. Soc.* **1983**, *105*, 7512.

- (3) Pearson, R. G. *J. Am. Chem. Soc.* **1985**, *107*, 6801.
- (4) Pearson, R. G. *J. Chem. Educ.* **1987**, *64*, 561.
- (5) Parr, R. G.; Yang, W. *Density Functional Theory of Atoms and Molecules*; Oxford University Press: New York, 1989.
- (6) Dreizler, R. M.; Gross, E. K. V. *Density Functional Theory*; Springer: Berlin, 1990.
- (7) Chattaraj, P. K.; Nath, S.; Sannigrahi, A. B. *J. Phys. Chem.* **1994**, *98*, 9143.
- (8) Cárdenas-Jirón, G. I.; Lahsen, J.; Toro-Labbé, A. *J. Phys. Chem.* **1995**, *99*, 5325.
- (9) Cárdenas-Jirón, G. I.; Toro-Labbé, A. *J. Phys. Chem.* **1995**, *99*, 12730.
- (10) Chattaraj, P. K.; Nath, S.; Sannigrahi, A. B. *Chem. Phys. Lett.* **1993**, *212*, 223.
- (11) Hammond, G. S. *J. Am. Chem. Soc.* **1955**, *77*, 334.
- (12) Parr, R. G.; Chattaraj, P. K. *J. Am. Chem. Soc.* **1991**, *113*, 1854.
- (13) Chattaraj, P. K.; Liu, G. H.; Parr, R. G. *Chem. Phys. Lett.* **1995**, *237*, 171.
- (14) Pearson, R. G.; Palke, W. E. *J. Phys. Chem.* **1992**, *96*, 3283.
- (15) Gázquez, J. L.; Martínez, A.; Méndez, F. *J. Phys. Chem.* **1993**, *97*, 4059.
- (16) Nath, S.; Sannigrahi, A. B.; Chattaraj, P. K. *J. Mol. Struct. (THEOCHEM)* **1994**, *309*, 65.
- (17) Willis, C.; Back, R. A. *Can. J. Chem.* **1973**, *51*, 3605.
- (18) Blau, E. J.; Hochheimer, B. F. *J. Chem. Phys.* **1964**, *41*, 1174.
- (19) Rosengren, K.; Pimentel, G. C. *J. Chem. Phys.* **1965**, *43*, 507.
- (20) Trombetti, A. *Can. J. Phys.* **1968**, *46*, 1005.
- (21) Bondybey, V. E.; Nibler, J. W. *J. Chem. Phys.* **1973**, *58*, 2125.
- (22) Winter, N. W.; Pitzer, R. M. *J. Chem. Phys.* **1975**, *62*, 1269.
- (23) Spears, L. G., Jr.; Hutchinson, J. S. *J. Chem. Phys.* **1988**, *88*, 240.
- (24) Spears, L. G., Jr.; Hutchinson, J. S. *J. Chem. Phys.* **1988**, *88*, 250.
- (25) Coxon, J. M.; McDonald, D. Q. *Tetrahedron Lett.* **1992**, *33*, 3673.
- (26) Cimiriaglia, R.; Hofmann, H. J. *Chem. Phys. Lett.* **1994**, *217*, 430.
- (27) Angeli, C.; Cimiriaglia, R.; Hofmann, H. J. *Chem. Phys. Lett.* **1996**, *259*, 276.
- (28) Kohn, W.; Becke, A. D.; Parr, R. G. *J. Phys. Chem.* **1996**, *100*, 12974 and references therein.
- (29) Cárdenas-Jirón, G. I.; Toro-Labbé, A. *J. Mol. Struct. (THEOCHEM)*, **1997**, *390*, 79.
- (30) Chattaraj, P. K.; Nath, S. *Int. J. Quantum Chem.* **1994**, *49*, 705.
- (31) Chattaraj, P. K.; Nath, S. *Chem. Phys. Lett.* **1994**, *217*, 342.
- (32) Marcus, R. A. *Annu. Rev. Phys. Chem.* **1964**, *15*, 155.
- (33) Cárdenas-Jirón, G. I.; Toro-Labbé, A.; Bock, Ch. W.; Maruani, J. In *Structure and Dynamics of Non-Rigid Molecular Systems*; Smeyers, Y. G., Ed.; Kluwer Academic: Dordrecht, 1995; pp 97–120, and references therein.
- (34) Cárdenas-Jirón, G. I.; Cárdenas-Lailhacar, C.; Toro-Labbé, A. *J. Mol. Struct. (THEOCHEM)*, **1990**, *210*, 279.
- (35) Cárdenas-Lailhacar, C.; Toro-Labbé, A. *Theor. Chim. Acta* **1990**, *76*, 411.
- (36) Zhou, Z.; Parr, R. G. *J. Am. Chem. Soc.* **1990**, *112*, 5720.
- (37) Spartan version 4.1; Wavefunction Inc.: 18401 Von Karman Ave., #370, Irvine, CA 92715.
- (38) Jursic, B. S. *Chem. Phys. Lett.* **1996**, *261*, 13.